

# Angular truncation errors in integrating nephelometry

Hans Moosmüller<sup>a)</sup> and W. Patrick Arnott

*Desert Research Institute, University of Nevada System, 2215 Raggio Parkway, Reno, Nevada 89512*

(Received 16 August 2002; accepted 4 March 2003)

Ideal integrating nephelometers integrate light scattered by particles over all directions. However, real nephelometers truncate light scattered in near-forward and near-backward directions below a certain truncation angle (typically  $7^\circ$ ). This results in truncation errors, with the forward truncation error becoming important for large particles. Truncation errors are commonly calculated using Mie theory, which offers little physical insight and no generalization to nonspherical particles. We show that large particle forward truncation errors can be calculated and understood using geometric optics and diffraction theory. For small truncation angles (i.e.,  $<10^\circ$ ) as typical for modern nephelometers, diffraction theory by itself is sufficient. Forward truncation errors are, by nearly a factor of 2, larger for absorbing particles than for nonabsorbing particles because for large absorbing particles most of the scattered light is due to diffraction as transmission is suppressed. Nephelometers calibration procedures are also discussed as they influence the effective truncation error. © 2003 American Institute of Physics. [DOI: 10.1063/1.1581355]

## I. INTRODUCTION

An ideal integrating nephelometer integrates light scattered by an aerosol over all directions, that is over  $4\pi$  steradians.<sup>1–5</sup> The total extinction is a sum of scattering into  $4\pi$  steradians and the extinction due to absorption. If the aerosol's refractive index is a real number, it exhibits no absorption and all extinction is caused by the scattered light.

Real nephelometers are not ideal, but introduce various systematic errors influencing the measured value.<sup>6–8</sup> In particular, a fraction of the near-forward and near-backward scattered light is not measured. This is known as angular truncation error  $T$ , which is a function of the truncation angle  $\alpha$  (typical value:  $\alpha = 7^\circ$ ). For particles large compared to the wavelength of the scattered light, this truncation error is generally larger than other systematic measurement errors and can become as large as a factor of 2. While truncation errors have been discussed previously,<sup>4,9–14</sup> understanding of this phenomenon is still limited. Additional angular nonidealities,<sup>7</sup> which may arise from the use of a non-Lambertian diffuser, are not included in this discussion.

In this article, truncation errors for homogeneous, spherical particles are calculated using Mie theory for a matrix of size parameters and truncation angles. The refractive index of the surrounding medium is taken to be unity, appropriate when considering particles in the atmosphere. Extension to other real refractive indices for the surrounding medium is trivial. A physical explanation of features that occur in the exact Mie theory is given for several limiting cases using Rayleigh scattering, diffraction, reflection, and transmission theory. Comparison of these approximate results with Mie theory outlines the size parameters and truncation angles at which the various approximations are useful. None of our calculations considers the particle size distributions or

the bandwidth of the nephelometer wavelength response, but instead results are given as function of size parameter. This furthers direct physical understanding and not much is lost in terms of direct applicability, as size distribution and wavelength response have to be tailored to the aerosol and nephelometer characteristics, respectively. As truncation errors can occur during both nephelometer calibration and use, calibration procedures and their influence on truncation errors are also discussed.

Ideally nephelometer truncation angles should be reduced well below the common truncation angle of  $7^\circ$  to facilitate the accurate measurement of total scattering from coarse particles. In practice, no significant improvements have been made over the last few decades. As a consequence these conventional nephelometers (such as the TSI 3563) are well suited for the measurement of total scattering from accumulation mode particles (i.e., volume mean diameters between 0.2 and 0.4  $\mu\text{m}$ ) with nonidealities introducing uncertainties less than 10%.<sup>6</sup> However, for coarse particles (diameters greater 1  $\mu\text{m}$ ) these errors increase dramatically to 20%–50%,<sup>6</sup> indicating that these nephelometer are not well suited for the measurement of total scattering from coarse particles. Very recently, an integrating sphere integrating nephelometer with truncation angles of  $1^\circ$  has been developed.<sup>15</sup> Truncation losses for this nephelometer are less than 25% for nonabsorbing particles with diameters below 16  $\mu\text{m}$ , making it well suited for the measurement of total scattering from ambient coarse particles.

In practice, some nephelometers yield measurements at multiple wavelengths, which may be useful for the correction of truncation errors. It has been shown, for field measurements at a coastal station, that truncation errors for sub- $\mu\text{m}$  particles are small and well correlated with the wavelength dependence of the scattering, while truncation errors for super- $\mu\text{m}$  particles are large and poorly correlated with the wavelength dependence.<sup>8</sup> Therefore, correction of truncation errors from multiwavelength nephelometers data seems fea-

<sup>a)</sup>Author to whom correspondence should be addressed; electronic mail: hansm@dri.edu

sible only for sub- $\mu\text{m}$  particles. The calculations in this publication and the resulting understanding also fully apply to near-forward scattering errors in extinction measurements. Here, a certain angular part of the near-forward scattering is included in the measurement of transmitted beam power, thereby indicating an extinction that is less than the actual extinction.

For incoherent scattering from  $j$  identical particles randomly located within a scattering volume  $V$ , uniformly illuminated with irradiance  $I_0$ , the power  $dP_{\text{Sca}}(\theta, \varphi)/d\Omega$  scattered into the solid angle  $d\Omega$  at a scattering angle  $\theta$  and an azimuthal angle  $\varphi$ , can be written as

$$\frac{dP_{\text{Sca}}(\theta, \varphi)}{d\Omega} = jI_0 \frac{dC_{\text{Sca}}(\theta, \varphi)}{d\Omega} = jI_0 C_{\text{Sca}} p(\theta, \varphi), \quad (1a)$$

where  $dC_{\text{Sca}}(\theta, \varphi)/d\Omega$  is the differential scattering cross section,  $C_{\text{Sca}}$  is the scattering cross section (the differential scattering cross section integrated over  $4\pi$  steradians), and  $p(\theta, \varphi)$  is the scattering phase function that describes the angular distribution of the scattered power. Equation (1a) implies that the phase function is normalized to one:

$$\int_{4\pi} d\Omega p(\theta, \varphi) = 1. \quad (1b)$$

(Note that normalization of phase functions to  $4\pi$  is also in common use.) In addition to scattering cross sections  $C_{\text{Sca}}$  (dimension of area), we use scattering coefficients  $\sigma$  (dimension of inverse distance) for ensembles of particles, where

$$\sigma = \frac{j}{V} C_{\text{Sca}}. \quad (2)$$

The fractional forward (backward) truncation error  $T_F(T_B)$  is the power  $P_F(\alpha_F)[P_B(\alpha_B)]$  of the light near-forward (backward) scattered into a cone with half-angle  $\alpha_F(\alpha_B)$  (this is the truncation angle) as a fraction of the total (into  $4\pi$  steradians) scattered power  $P_{4\pi}$  and can be written as

$$\begin{aligned} T_F(\alpha_F) &= \frac{P_F(\alpha_F)}{P_{4\pi}} = \frac{\int_0^\alpha d\theta \sin \theta \int_0^{2\pi} d\varphi \frac{dP_{\text{Sca}}(\theta, \phi)}{d\Omega}}{\int_0^\pi d\theta \sin \theta \int_0^{2\pi} d\varphi \frac{dP_{\text{Sca}}(\theta, \phi)}{d\Omega}} \\ &= \int_0^\alpha d\theta \sin \theta \int_0^{2\pi} d\varphi p(\theta, \varphi) \end{aligned} \quad (3a)$$

and

$$\begin{aligned} T_B(\alpha_B) &= \frac{P_B(\alpha_B)}{P_{4\pi}} = \frac{\int_{\pi-\alpha_B}^\pi d\theta \sin \theta \int_0^{2\pi} d\varphi \frac{dP_{\text{Sca}}(\theta, \phi)}{d\Omega}}{\int_0^\pi d\theta \sin \theta \int_0^{2\pi} d\varphi \frac{dP_{\text{Sca}}(\theta, \phi)}{d\Omega}} \\ &= \int_{\pi-\alpha_B}^\pi d\theta \sin \theta \int_0^{2\pi} d\varphi p(\theta, \varphi). \end{aligned} \quad (3b)$$

Defining the phase function  $p(\theta)$  as the result of the integration over the azimuthal angle  $\varphi$  in Eqs. (3), these equations simplify to

$$T_F(\alpha_F) = 2\pi \int_0^\alpha d\theta p(\theta) \sin \theta, \quad (4a)$$

$$T_B(\alpha_B) = 2\pi \int_{\pi-\alpha_B}^\pi d\theta p(\theta) \sin \theta. \quad (4b)$$

The integrals in Eqs. (4) need to be evaluated with phase functions obtained for particles of different size and refractive index. Particle size is expressed as the size parameter  $x$ , the ratio of particle circumference  $\pi d$  to optical wavelength  $\lambda$ :

$$x = \frac{\pi d}{\lambda}, \quad (5)$$

where  $d$  is the particle diameter. The refractive index  $m$  is a complex number with a real component  $n$ , responsible mainly for refraction and reflection and an imaginary component  $k$ , responsible mainly for absorption with

$$m = n + ik, \quad (6)$$

where the bulk absorption coefficient is  $4\pi k/\lambda$ .

## II. NEPHELOMETER CALIBRATION

Most of this article is concerned with the calculation of truncation errors with Eqs. (4). These calculations would be sufficient if nephelometers could directly measure the truncated scattering coefficient  $\sigma(\alpha_F, \alpha_B)$ , the scattering coefficient within their acceptance angles

$$\begin{aligned} \sigma(\alpha_F, \alpha_B) &= \sigma \int_{\alpha_F}^{\pi-\alpha_B} d\theta \sin(\theta) \int_0^{2\pi} d\varphi p(\theta, \varphi) \\ &= \sigma [1 - T_F(\alpha_F) - T_B(\alpha_B)] \\ &\equiv \sigma F(\alpha_F, \alpha_B), \end{aligned} \quad (7)$$

where  $\sigma = \sigma(\alpha_F = 0, \alpha_B = 0)$  is the total scattering coefficient one would like to measure and  $F(\alpha_F, \alpha_B)$  is called the truncation function.

However, real nephelometers do not directly measure  $\sigma(\alpha_F, \alpha_B)$  but give a signal  $S$  that is some function of  $\sigma(\alpha_F, \alpha_B)$ . This relationship can be expressed for small scattering coefficients in the form of a Taylor expansion as

$$\begin{aligned} S(\sigma(\alpha_F, \alpha_B)) &= S(0) + \frac{\sigma(\alpha_F, \alpha_B)}{1!} S'(0) \\ &\quad + \frac{\sigma^2(\alpha_F, \alpha_B)}{2!} S''(0) + \dots \\ &\quad + \frac{\sigma^n(\alpha_F, \alpha_B)}{n!} S^{(n)}(0) + \dots \end{aligned} \quad (8a)$$

For typical nephelometers, the linear part of the expansion [Eq. (8a)] describes the signal  $S$  accurately enough over the entire measurement range, resulting in

$$S(\sigma(\alpha_F, \alpha_B)) = W + K\sigma(\alpha_F, \alpha_B), \quad (8b)$$

where  $W = S(0)$  is the signal offset caused mostly by wall scattering and  $K = S'(0)$  is called the gain coefficient. To obtain values of  $W$  and  $K$ , the nephelometer is calibrated

with two media: one with small  $\sigma(\alpha_F, \alpha_B)$  termed  $\sigma_1(\alpha_F, \alpha_B)$  and one with relatively large  $\sigma(\alpha_F, \alpha_B)$  [still satisfying the approximations of Eqs. (8a) and (8b)] termed  $\sigma_2(\alpha_F, \alpha_B)$ . Calibration media are commonly gases (e.g., zero air and carbon dioxide), but aerosols and solids can also be used.<sup>4,6,16–18</sup> The nephelometer signal is measured with both media sequentially, yielding two signals (one for each medium),  $S_1$  and  $S_2$ :

$$S_{1,2}(\alpha_{F\_Neph}, \alpha_{B\_Neph}) = W + K\sigma_{1,2}(\alpha_{F\_Coeff}, \alpha_{B\_Coeff}), \quad (8c)$$

where we distinguish between the actual truncation angles  $\alpha_{F\_Neph}$  and  $\alpha_{B\_Neph}$  and the truncation angles  $\alpha_{F\_Coeff}$  and  $\alpha_{B\_Coeff}$  used to determine the truncated scattering coefficients  $\sigma(\alpha_{F\_Coeff}, \alpha_{B\_Coeff})$ . The determination of the truncated scattering cross sections requires knowledge of the nephelometer truncation angles and the phase functions of the calibration media. From Eq. (8c), the calibration constants  $K$  and  $W$  are

$$K = \frac{S_1(\alpha_{F\_Neph}, \alpha_{B\_Neph}) - S_2(\alpha_{F\_Neph}, \alpha_{B\_Neph})}{\sigma_1(\alpha_{F\_Coeff}, \alpha_{B\_Coeff}) - \sigma_2(\alpha_{F\_Coeff}, \alpha_{B\_Coeff})} \quad (8d)$$

and

$$\begin{aligned} W &= S_1(\alpha_{F\_Neph}, \alpha_{B\_Neph}) - K\sigma_1(\alpha_{F\_Coeff}, \alpha_{B\_Coeff}) \\ &= S_1(\alpha_{F\_Neph}, \alpha_{B\_Neph}) - \sigma_1(\alpha_{F\_Coeff}, \alpha_{B\_Coeff}) \\ &\quad \times \frac{S_1(\alpha_{F\_Neph}, \alpha_{B\_Neph}) - S_2(\alpha_{F\_Neph}, \alpha_{B\_Neph})}{\sigma_1(\alpha_{F\_Coeff}, \alpha_{B\_Coeff}) - \sigma_2(\alpha_{F\_Coeff}, \alpha_{B\_Coeff})}. \end{aligned} \quad (8e)$$

If the nephelometer is correctly calibrated with correctly truncated scattering coefficients  $\sigma_1$  and  $\sigma_2$  for its actual truncation angles, that is  $\alpha_{F\_Coeff} = \alpha_{F\_Neph}$  and  $\alpha_{B\_Coeff} = \alpha_{B\_Neph}$ , the truncated scattering coefficient  $\sigma_{Sample}(\alpha_{F\_Neph}, \alpha_{B\_Neph})$  for a sample can be obtained as

$$\sigma_{Sample}(\alpha_{F\_Neph}, \alpha_{B\_Neph}) = \frac{S_{Sample}(\alpha_{F\_Neph}, \alpha_{B\_Neph}) - W}{K}. \quad (9a)$$

If the phase function for the sample is known, the scattering

coefficient of the sample  $\sigma_{Sample} = \sigma_{Sample}(\alpha_{F\_Neph} = 0, \alpha_{B\_Neph} = 0)$  can be calculated with Eq. (7) as

$$\begin{aligned} \sigma_{Sample} &= \sigma_{Sample}(\alpha_{F\_Neph} = 0, \alpha_{B\_Neph} = 0) \\ &= \frac{\sigma_{Sample}(\alpha_{F\_Neph}, \alpha_{B\_Neph})}{F_{Sample}(\alpha_{F}, \alpha_{B})}. \end{aligned} \quad (9b)$$

If a gas is used for calibration, its phase function is the well-known Rayleigh phase function. For homogeneous, spherical calibration aerosols with known size distributions and refractive indices, phase functions can be readily calculated using Mie theory. Truncation angles for integrating nephelometers are commonly known and therefore the truncated scattering coefficient  $\sigma_{Sample}(\alpha_{F\_Neph}, \alpha_{B\_Neph})$  for a sample can be obtained from Eq. (9a). The last step, obtaining the integrated scattering coefficient  $\sigma_{Sample} = \sigma_{Sample}(\alpha_{F\_Neph} = 0, \alpha_{B\_Neph} = 0)$  from Eq. (9b), is unfortunately often impossible as the effective phase function of a sample aerosol is generally unknown. Possible solutions to this problem include using a nephelometer with small truncation angle, measuring or estimating the aerosol size distribution and calculating the phase function, measuring the phase function with a polar nephelometer, or using a polar nephelometer instead of an integrating nephelometer in the first place.<sup>19</sup> However, polar nephelometers have related systematic errors depending on their angular resolution and truncation errors.<sup>20</sup>

This should be the end of the calibration story. However, it seems to be common practice to neglect calibration truncation errors and to use  $\sigma(0,0) = \sigma(\alpha_{F\_Coeff} = 0, \alpha_{B\_Coeff} = 0)$  instead of  $\sigma(\alpha_{F\_Coeff}, \alpha_{B\_Coeff})$  in Eqs. (8d) and (8e) to determine  $K$  and  $W$ , even if  $\alpha_{F\_Neph} \neq 0$  and  $\alpha_{B\_Neph} \neq 0$ . This practice may be justified if a nephelometer has small truncation angles and calibration media, without pronounced near forward and near backward scattering peaks, e.g., gases are used. In this case, neglecting the calibration truncation error may not decrease nephelometer accuracy significantly.<sup>6</sup> If calibration truncation errors are neglected (i.e.,  $\alpha_{F\_Coeff} = \alpha_{B\_Coeff} = 0$ ), the calibration procedure yields coefficients  $K_0$  and  $W_0$  instead of the true values of  $K$  and  $W$  where

$$k_0 = \frac{S_1(\alpha_{F\_Neph}, \alpha_{B\_Neph}) - S_2(\alpha_{F\_Neph}, \alpha_{B\_Neph})}{\sigma_1(\alpha_{F\_Coeff} = 0, \alpha_{B\_Coeff} = 0) - \sigma_2(\alpha_{F\_Coeff} = 0, \alpha_{B\_Coeff} = 0)} \quad (10a)$$

and

$$\begin{aligned} W_0 &= S_1(\alpha_{F\_Neph}, \alpha_{B\_Neph}) \\ &\quad - K_0\sigma_1(\alpha_{F\_Coeff} = 0, \alpha_{B\_Coeff} = 0). \end{aligned} \quad (10b)$$

Measuring the scattering coefficient of a sample with a nephelometer calibrated using the calibration constants  $K_0$  and  $W_0$  instead of  $K$  and  $W$  yields a scattering coefficient  $\sigma_{Sample_0}$  of the sample as

$$\begin{aligned} \sigma_{Sample_0} &= \frac{S_{Sample}(\alpha_{F\_Neph}, \alpha_{B\_Neph}) - W_0}{K_0} \\ &= \sigma_1(0,0)[1 + S_{Ratio}] - \sigma_2(0,0)S_{Ratio}, \end{aligned} \quad (11a)$$

where  $S_{Ratio}$  is defined as

$$S_{Ratio} = \frac{S_{Sample}(\alpha_{F\_Neph}, \alpha_{B\_Neph}) - S_1(\alpha_{F\_Neph}, \alpha_{B\_Neph})}{S_1(\alpha_{F\_Neph}, \alpha_{B\_Neph}) - S_2(\alpha_{F\_Neph}, \alpha_{B\_Neph})}. \quad (11b)$$

Using Eq. (7) to replace  $\sigma(0,0)$  by  $\sigma(\alpha_{F\_Neph}, \alpha_{B\_Neph})/F(\alpha_{F\_Neph}, \alpha_{B\_Neph})$  yields

$$\sigma_{Sample\_0} = \frac{\sigma_1(\alpha_{F\_Neph}, \alpha_{B\_Neph})}{F_1(\alpha_{F\_Neph}, \alpha_{B\_Neph})} [1 + S_{Ratio}] - \frac{\sigma_2(\alpha_{F\_Neph}, \alpha_{B\_Neph})}{F_2(\alpha_{F\_Neph}, \alpha_{B\_Neph})} S_{Ratio}. \quad (11c)$$

If the sum of the fractional forward and backward truncation errors are identical for calibration media 1 and 2, e.g., using two calibration gases,  $F_1(\alpha_{F\_Neph}, \alpha_{B\_Neph}) = F_2(\alpha_{F\_Neph}, \alpha_{B\_Neph}) [= F_{Cal}(\alpha_{F\_Neph}, \alpha_{B\_Neph})]$ , and  $\sigma_{Sample\_0}$  can be related to  $\sigma_{Sample}$  as

$$\sigma_{Sample\_0} = \frac{\sigma_{Sample}(\alpha_{F\_Neph}, \alpha_{B\_Neph})}{F_{Cal}(\alpha_{F\_Neph}, \alpha_{B\_Neph})} = \frac{F_{Sample}(\alpha_{F\_Neph}, \alpha_{B\_Neph})}{F_{Cal}(\alpha_{F\_Neph}, \alpha_{B\_Neph})} \sigma_{Sample}. \quad (11d)$$

Equation (11d) confirms the common physical understanding that if one calibrates a nephelometer with two gases (identical truncation errors), without considering calibration truncation errors, the nephelometer is correctly calibrated to measure the un-truncated scattering coefficient of a gaseous sample. In Eq. (11d) this corresponds to  $F_{Cal} = F_{Sample}$ , resulting in  $\sigma_{Sample\_0} = \sigma_{Sample}$ . In conclusion, to understand nephelometer calibrations and to correctly interpret nephelometer measurements, one needs to be aware of the phase functions for the calibration media, the nephelometer truncation angles, and if the calibration procedure has accounted for the resulting calibration truncation errors.

### III. MIE THEORY

Light scattering and absorption by homogeneous spherical particles is described by Mie theory.<sup>21</sup> With the ready availability of powerful personal computers and Mie codes,<sup>22,23</sup> numerical solutions to scattering problems involving homogeneous spherical particles can be readily calculated. However, approximate solutions of scattering problems are still valuable to gain a physical understanding of the scattering process and for generalization to nonspherical particles.<sup>24,25</sup>

To evaluate the truncation errors  $T_F(\alpha)$  and  $T_B(\alpha)$ , first the Mie phase function  $p_{Mie}(\theta)$  is evaluated for different size parameters  $x$  and refractive indices with the Mie code BHMIE.<sup>23</sup> The phase function was calculated for one thousand (1000) values of the size parameter  $x$ , chosen to be equidistant on a logarithmic scale, ranging from very small ( $x=0.1$ ; e.g.,  $d=0.0175 \mu\text{m}$  at  $\lambda=0.55 \mu\text{m}$ ) to very large ( $x=1000$ ; e.g.,  $d=175 \mu\text{m}$  at  $\lambda=0.55 \mu\text{m}$ ) particles. The extreme sizes were chosen to show the convergence of results obtained from Mie theory with those obtained from geometric optics plus diffraction for very large particles and with those obtained from Rayleigh theory for very small particles. Optically very small particles are commonly found in the nuclei mode,<sup>26</sup> and very large particles may be found in

clouds, albeit generally not in spherical shape.<sup>27</sup> The phase function was calculated for scattering angles  $\theta$  ranging from  $0^\circ$  to  $180^\circ$ . To resolve the sharp near-forward scattering lobe for large  $x$ , an angular resolution for  $\theta$  of  $0.025^\circ$  was used. Refractive indices representative for dry atmospheric aerosol were chosen as  $m_{non-abs}=(1.50,0.0)$  for nonabsorbing aerosol, and  $m_{abs}=(1.50,0.5)$  for light absorbing aerosol. The integrations in Eqs. (4) were solved numerically using a five-point Newton-Cotes integration formula yielding the forward and backward truncation errors  $T_F(\alpha, x)$  and  $T_B(\alpha, x)$ , which are shown in Figs. 1(a)–1(d) for  $m_{non-abs}$  and  $m_{abs}$ .

One notes that for very small particles, forward and backward truncation errors are identical and independent of the refractive index used (i.e., Rayleigh regime). They increase gradually from  $\sim 0$  at small angles to 0.5 at  $90^\circ$ . For larger nonabsorbing particles the truncation errors exhibit significant oscillations as a function of particle size—these oscillations are strongly damped for absorbing particles. For large ( $x \geq 100$ ) nonabsorbing particles, the forward truncation error increases from 0 at  $0^\circ$  to about 0.5 at very small angles (i.e.,  $< 2^\circ$ ), then slowly and gradually increases to near 1 at  $90^\circ$ . For large ( $x \geq 100$ ) absorbing particles, the forward truncation error increases from 0 at  $0^\circ$  to near 1 at very small angles, then remains near constant and increases only very slowly for larger angles. For large particles ( $x \geq 1$ ) forward truncation errors  $T_F$  are much larger than backward truncation errors  $T_B$ , as evident from Figs. 1(a)–1(d) and from the  $T_F/T_B$  ratios shown in Figs. 1(e) and 1(f). Because truncation errors can largely be neglected for small particles, the article focuses on the dominant forward truncation errors. In the following, the properties as described above and shown in Fig. 1 are discussed in the context of both the small particle and the large particle approximations.

### IV. SMALL PARTICLE APPROXIMATION (RAYLEIGH REGIME)

For small particles ( $x \ll 1$ ), the scattering can be described by the Rayleigh approximation. The phase function in this regime can be expressed as

$$p_{Ray}(\theta) = \frac{3}{16\pi} (1 + \cos^2 \theta). \quad (12)$$

This phase function can be integrated analytically and yields identical forward and backward Rayleigh truncation errors  $T_{Ray}$  with

$$T_{Ray}(\alpha) = T_{F\_R}(\alpha) = T_{B\_R}(\alpha) = \frac{1}{2} [1 - \frac{1}{4} (3 \cos \alpha + \cos^3 \alpha)]. \quad (13)$$

This functional dependence of Rayleigh truncation errors on the cutoff angle  $\alpha$  is shown in Fig. 2. In this small particle Rayleigh approximation, the truncation errors are independent of refractive index and particle size. Truncation errors in the Rayleigh regime are quite small for typical nephelometer truncation angles [e.g.,  $T_{Ray}(7^\circ) = 0.56\%$ ]. In addition, these

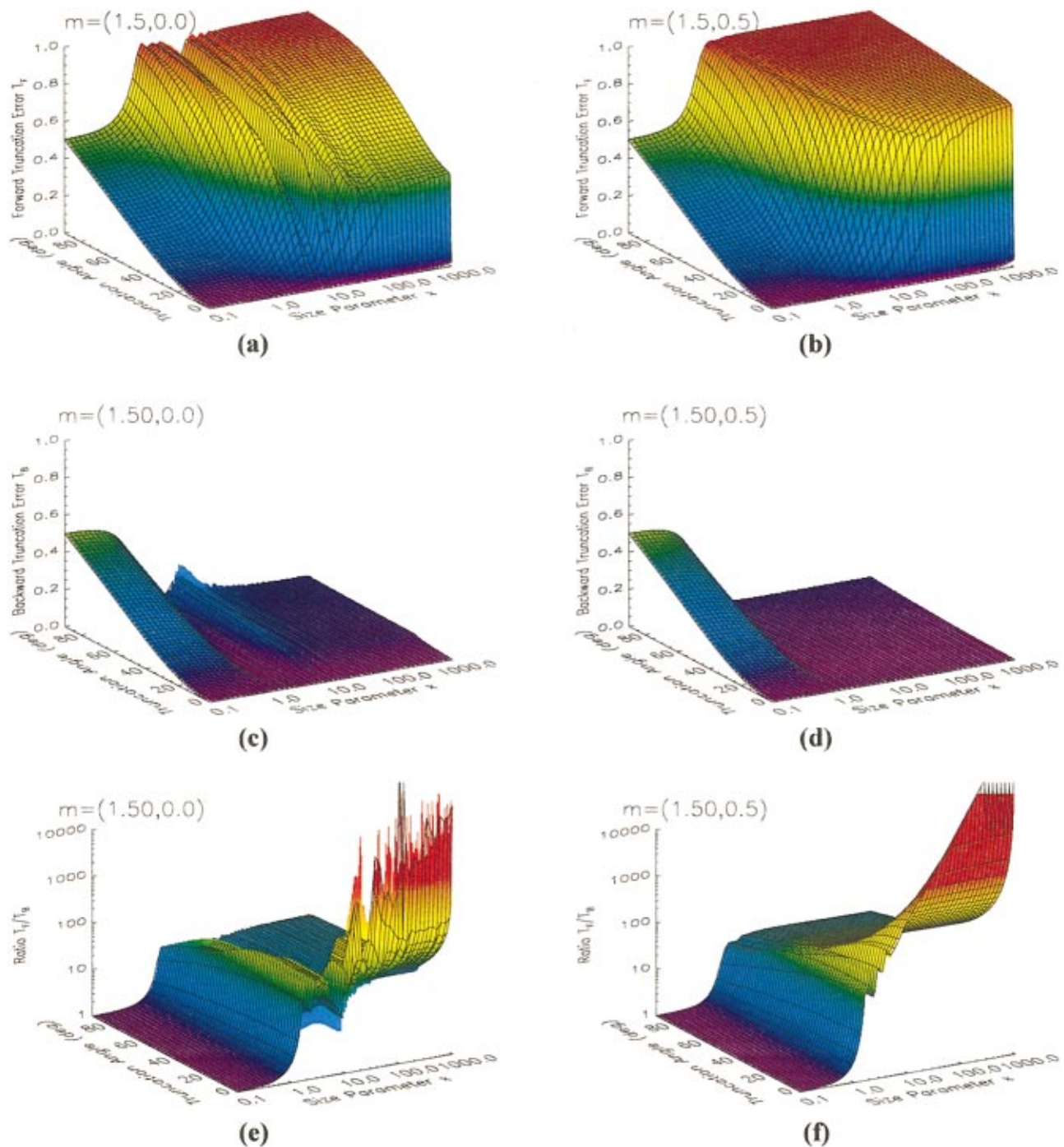


FIG. 1. (Color) Truncation error from Mie theory as function of size parameter  $x$  and truncation angle  $\alpha$ : (a) forward direction, nonabsorbing particles; (b) forward direction, absorbing particles; (c) backward direction, nonabsorbing particles; (d) backward direction, absorbing particles; (e) ratio of forward and backward directions, nonabsorbing particles; and (f) ratio of forward and backward directions, absorbing particles.

errors can be eliminated through the calibration procedure if the nephelometer has been calibrated with gases, which is the most common calibration procedure.

Note that Eq. (12) [and consequently Eq. (13)] is exact only for spherical scatterers as appropriate for comparison with Mie theory. An equation for the phase function of anisotropic molecules has been given by Chandrasekhar.<sup>28</sup> The application of this equation to air has been discussed by Bucholtz.<sup>29</sup> For the nonspherical molecules making up the majority of air, Eq. (4) is in error by typically less than 1.5%.

## V. LARGE PARTICLE APPROXIMATION

For a particle very large compared to the wavelength ( $x \gg 1$ ), the total extinction cross section  $C_{\text{Ext}}$  is twice the geometric cross section  $G$  ( $C_{\text{Ext}} = 2G = 0.5 \pi d^2$ ). All energy incident on the geometric cross section of a particle is scattered or absorbed, i.e., in any way removed from the proceeding wave. This gives an effective extinction cross-section equal to  $G$ , the geometric area. In addition, diffraction forms an angular pattern that is identical to the

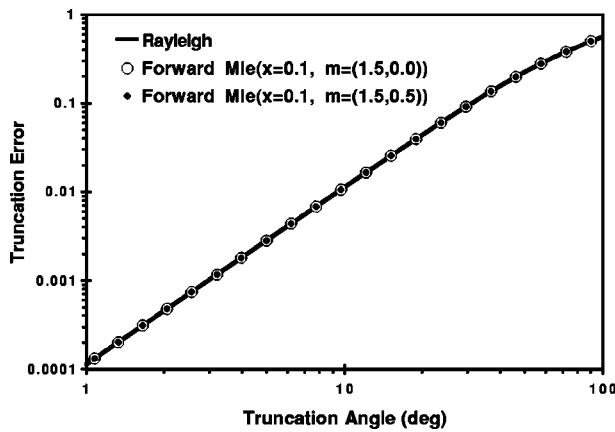


FIG. 2. Very small ( $x=0.1$ ; e.g.,  $d=0.0175 \mu\text{m}$  at  $\lambda=0.55 \mu\text{m}$ ) particle truncation error from Mie and Rayleigh theories.

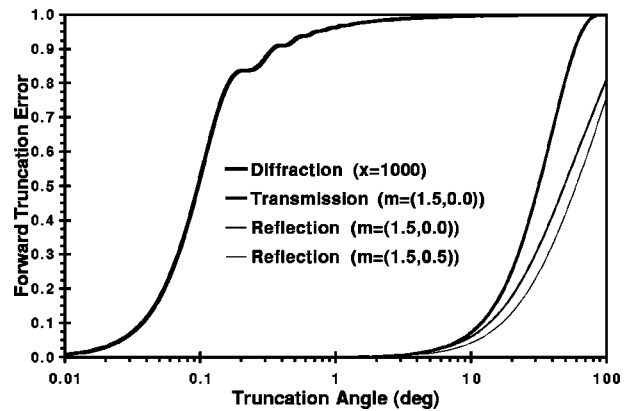


FIG. 3. Forward scattering truncation errors for diffraction, transmission, and reflection as individual processes for very large ( $x=1000$ ; e.g.,  $d = 175 \mu\text{m}$  at  $\lambda=0.55 \mu\text{m}$ ) particles. Note that the lines are in the same order as shown in the legend.

diffraction through a hole of area  $G$  by Babinet's principle. This gives diffraction (i.e., near-forward scattering) again with a cross section  $G$ . The total extinction cross section is therefore the sum of the two, equal to  $2G$  in the large particle limit.<sup>30</sup> The total scattering cross section  $C_{\text{Sca}} = \tilde{\omega}_0 C_{\text{Ext}} = 2\tilde{\omega}_0 G$  depends on the single-scattering albedo  $\tilde{\omega}_0 = C_{\text{Sca}}/C_{\text{Ext}}$  of the particle.

The phase function in the large particle approximation  $p_{\text{LP}}$  can be written as the sum of the transmission, reflection, and diffraction phase functions (i.e.,  $p_T, p_R, p_D$ , respectively), each weighted by the contribution of the respective process to the total scattering cross section, as

$$p_{\text{LP}} = \frac{C_{\text{Sca}_T}}{C_{\text{Sca}}} p_T + \frac{C_{\text{Sca}_R}}{C_{\text{Sca}}} p_R + \frac{C_{\text{Sca}_D}}{C_{\text{Sca}}} p_D \quad (14a)$$

and consequently the forward truncation error in the large particle approximation  $T_{F\_LP}$  becomes

$$T_{F\_LP} = \frac{C_{\text{Sca}_T}}{C_{\text{Sca}}} T_{F\_T} + \frac{C_{\text{Sca}_R}}{C_{\text{Sca}}} T_{F\_R} + \frac{C_{\text{Sca}_D}}{C_{\text{Sca}}} T_{F\_D}, \quad (14b)$$

with

$$C_{\text{Sca}} = C_{\text{Sca}_T} + C_{\text{Sca}_R} + C_{\text{Sca}_D}, \quad (14c)$$

where all phase functions are properly normalized to one [see Eq. (1b)]. Equations (14) represent an approximation that neglects the interference between transmitted, reflected, and diffracted light.<sup>31</sup> Phase functions for scattering due to transmission, reflection, and diffraction from spheres with complex refractive index have been given in the form of a "gain" by Liou and Hansen.<sup>32</sup> Note however, that their expressions for  $u$  and  $v$  [in their Eq. (7)] contain a typographical error; the correct expressions are shown as part of Eq. (2.10) in Hansen and Travis.<sup>33</sup>

### A. Scattering due to external reflection

The phase function for scattering due to external reflection from spheres with complex refractive index can be written as<sup>32</sup>

$$p_R = \frac{C_{\text{Sca}}}{2\tilde{\omega}_0 C_{\text{Sca}_R}} \frac{1}{8\pi} \left\{ \left( \frac{[\sin(\theta/2) - u_R]^2 + v_R^2}{[\sin(\theta/2) - u_R]^2 + v_R^2} \right) + \left( \frac{[(n^2 - k^2)\sin(\theta/2) - u_R]^2 + [2nk\sin(\theta/2) - v_R]^2}{[(n^2 - k^2)\sin(\theta/2) + u_R]^2 + [2nk\sin(\theta/2) + v_R]^2} \right) \right\}, \quad (15a)$$

where  $C_{\text{Sca}}/(2\tilde{\omega}_0)$  is the geometric cross section  $G$  of the particle, the two fractions in round brackets contain the  $s$ - and  $p$ -polarized contributions, respectively, and  $u_R$  and  $v_R$  can be expressed as

$$u_R = \sqrt{\frac{(n^2 - k^2 - \cos^2(\theta/2)) + \sqrt{(n^2 - k^2 - \cos^2(\theta/2))^2 + (2nk)^2}}{2}}, \quad (15b)$$

$$v_R = \sqrt{\frac{-(n^2 - k^2 - \cos^2(\theta/2)) + \sqrt{(n^2 - k^2 - \cos^2(\theta/2))^2 + (2nk)^2}}{2}}. \quad (15c)$$

The scattering phase function  $p_R$  is independent of particle size. For nonabsorbing particles (i.e.,  $k=0$  and consequently  $\tilde{\omega}_0=1$ ), Eqs. (15) simplify considerably and the phase function becomes<sup>34</sup>

$$p_R(k=0) = \frac{C_{\text{Sca}}}{2C_{\text{Sca}_R}} \frac{1}{8\pi} \left\{ \left( \frac{\sin(\theta/2) - \sqrt{n^2 - \cos^2(\theta/2)}}{\sin(\theta/2) + \sqrt{n^2 - \cos^2(\theta/2)}} \right)^2 + \left( \frac{n^2 \sin(\theta/2) - \sqrt{n^2 - \cos^2(\theta/2)}}{n^2 \sin(\theta/2) + \sqrt{n^2 - \cos^2(\theta/2)}} \right)^2 \right\}, \quad (16)$$

where  $C_{\text{Sca}}/2$  is the geometric cross section  $G$  of the particle.

The resulting forward truncation error for external reflection is calculated from Eq. (4a) and can be seen in Fig. 3 for both nonabsorbing [i.e.,  $m_{\text{non-abs}}=(1.5,0.0)$ ] and absorbing [i.e.,  $m_{\text{abs}}=(1.5,0.5)$ ] particles. For all angles of interest (i.e.,  $\alpha \leq 90^\circ$ ), the forward truncation error for nonabsorbing particles is slightly larger than that for absorbing particles. At a typical truncation angle of  $7^\circ$ , the forward truncation error due to reflection  $T_{F\_R}$  is only a few percent, that is  $T_{F\_R}(m_{\text{non-abs}}, \alpha=7^\circ)=3.2\%$  and  $T_{F\_R}(m_{\text{abs}}, \alpha=7^\circ)=2.2\%$ . Note that this truncation error would be directly applicable only if reflection constituted the only scattering process. Therefore, Eq. (14b) must be used to calculate the compounded truncation error from all scattering processes.

## B. Scattering due to transmission with refraction

For particles with a small product of imaginary part  $k$  of the refractive index and size parameter  $x$  (i.e., small  $kx$ ), some of the light incident on the particle is refracted twice and transmitted, contributing to the scattering. In addition, some of the transmitted light undergoes internal reflections. For the refractive indices considered here, the contribution of internally reflected light to the total scattering cross section is on the order of a few percent or less. At certain scattering angles, internally reflected light can make a significant contribution leading to rainbows. However, scattering angles  $\theta$  for primary and secondary rainbows are larger than  $90^\circ$  for refractive indices of  $m > 1.116$  (primary rainbow) and  $m < 1.518$  (secondary rainbow) and therefore do not contribute to forward truncation errors for  $m_{\text{non-abs}}=(1.5,0.0)$ . Therefore, transmitted light that has undergone internal reflections can be neglected here.

Phase functions for transmitted light (including those corresponding to single or multiple internal reflections) can be found in Liou and Hansen.<sup>32</sup> However, we are not aware of an analytical form for any of these phase functions as a function of the scattering angle  $\theta$ . Instead, the angle  $\tau$  between incident beam and sphere surface is used most of the time. For light transmitted with refraction but without internal reflection, the scattering angle  $\theta$  can be written as a function of  $\tau$  as

$$\theta = 2 \left[ \arccos\left(\frac{1}{n} \cos \tau\right) - \tau \right] \quad (17)$$

with  $0 \leq \theta \leq 2 \arccos(1/n)$  for  $\pi/2 \geq \tau \geq 0$ . The phase function  $p_T$  for light transmitted with refraction but without internal reflection can be written as<sup>32</sup>

$$p_T = \frac{C_{\text{Sca}}}{2\tilde{\omega}_0 C_{\text{Sca}_R}} \frac{1}{4\pi} \frac{\sin \tau \cos \tau \left[ (1 - |r_1|^2)^2 + (1 - |r_2|^2)^2 \right]}{\sin \theta \left| 1 - \frac{\tan \tau}{\tan(\arccos(\cos \tau/n))} \right|} \times \exp \left\{ -4xk \sin \left[ \arccos\left(\frac{\cos \tau}{n}\right) \right] \right\}, \quad (18a)$$

where  $C_{\text{Sca}}/(2\tilde{\omega}_0)$  is the geometric cross section  $G$  of the particle,  $1 - |r_1|^2$  and  $1 - |r_2|^2$  contain the  $s$ - and  $p$ -polarized contributions, respectively, and  $|r_1|^2$  and  $|r_2|^2$  can be expressed as

$$|r_1|^2 = \frac{(\sin \tau - u_T)^2 + v_T^2}{(\sin \tau + u_T)^2 + v_T^2}, \quad (18b)$$

$$|r_2|^2 = \frac{((n^2 - k^2) \sin \tau - u_T)^2 + (2nk \sin \tau - v_T)^2}{((n^2 - k^2) \sin \tau + u_T)^2 + (2nk \sin \tau + v_T)^2}, \quad (18c)$$

where

$$u_T = \sqrt{\frac{(n^2 - k^2 - \cos^2 \tau) + \sqrt{(n^2 - k^2 - \cos^2 \tau)^2 + (2nk)^2}}{2}}, \quad (18d)$$

$$v_T = \sqrt{\frac{-(n^2 - k^2 - \cos^2 \tau) + \sqrt{(n^2 - k^2 - \cos^2 \tau)^2 + (2nk)^2}}{2}}. \quad (18e)$$

The scattering phase function  $p_T$  is independent of particle size only for nonabsorbing particles (i.e.,  $k=0$  and consequently  $\tilde{\omega}_0=1$ ). In this case, Eqs. (18) simplify considerably and the phase function becomes<sup>34</sup>

$$p_T(k=0) = \frac{C_{\text{Sca}}}{2C_{\text{Sca}_T}} \frac{2}{\pi} \left( \frac{n}{n^2 - 1} \right)^4 \times \frac{(n \cos(\theta/2) - 1)^3 (n - \cos(\theta/2))^3}{\cos(\theta/2) (n^2 + 1 - 2n \cos(\theta/2))^2} \times (1 + \sec^4(\theta/2)), \quad (19)$$

where in the final bracket the term “1” corresponds to the  $s$ -polarized and the term “ $\sec^4(\theta/2)$ ” to the  $p$ -polarized component.

The resulting forward truncation error for transmission is calculated from Eq. (4a) and can be seen in Fig. 3 for large nonabsorbing [i.e.,  $m_{\text{non-abs}}=(1.5,0.0)$ ] particles. No light is transmitted at angles  $\theta > 2 \arccos(1/n)$  [see Eq. (17)] and the truncation error for transmission is constant above this angle. For strongly absorbing (i.e.,  $kx > 2$ ) particles, virtually no light is transmitted due to the exponential factor in Eq. (18a)—in this case the extinction is due to diffraction, reflection, and absorption. Therefore, the contribution of transmission phase functions to truncation errors is negligible for strongly absorbing particles. For nonabsorbing particles [i.e.,  $m_{\text{non-abs}}=(1.5,0.0)$ ], the truncation error due to transmission is smaller than that due to reflection for  $\alpha \leq 3.1^\circ$ , while at larger angles of interest (i.e.,  $3.1^\circ \leq \alpha \leq 90^\circ$ ) it is larger. At a typical truncation angle of  $7^\circ$ , the forward truncation error due to transmission  $T_{F\_R}$  is only a few percent, i.e.,  $T_{F\_T}(m_{\text{non-abs}}, \alpha=7^\circ)=3.6\%$ . Note that this truncation error

would be directly applicable only if transmission constituted the only scattering process. Therefore, Eq. (14b) must be used to calculate the compounded truncation error from all scattering processes.

### C. Scattering due to diffraction

The near-forward scattering by large spherical particles ( $x \gg 1$ ) can be described in the far field by Kirchhoff diffraction theory for a circular aperture independent of the particle refractive index. (Obviously, this is not true if the particles refractive index equals that of the surrounding medium, i.e., in this case there is no “optical particle.”) The diffraction scattering cross section  $C_{Sca\_D}$  equals the geometric cross section and the diffraction phase function  $p_D$  can be written for large  $x$  as<sup>23</sup>

$$p_D(\theta) = \frac{1}{\pi} \left( \frac{1 + \cos \theta}{2} \right)^2 \left( \frac{J_1(x \sin \theta)}{\sin \theta} \right)^2, \quad (20)$$

where most of the scattered power is contained in the near forward direction. The forward truncation error for light scattered through diffraction  $T_{F\_D}$  [Eq. (4a)] becomes

$$\begin{aligned} T_{F\_D}(\alpha) &= \frac{P_{F\_D}(\alpha)}{P_{D\_4\pi}} \\ &= 2\pi \int_0^\alpha d\theta p_D(\theta) \sin(\theta) \\ &= 2 \int_0^\alpha d\theta \left( \frac{1 + \cos \theta}{2} \right)^2 \frac{[J_1(x \sin \theta)]^2}{\sin \theta}. \end{aligned} \quad (21a)$$

This integral can be solved analytically through substitution (i.e., for  $x \sin \theta$ ), use of common Bessel function identities, use of the product rule, and of the small angle approximation (i.e.,  $\cos \theta \approx 1 - \theta^2$  and  $\sec \theta \approx 1 + \theta^2$ ), yielding<sup>34</sup>

$$\begin{aligned} T_{F\_D}(x \sin \alpha) &= \frac{P_{F\_D}}{P_{D\_4\pi}} \\ &= 1 - [J_0^2(x \sin \alpha) + J_1^2(x \sin \alpha)]. \end{aligned} \quad (21b)$$

The forward truncation error for light scattered through diffraction  $T_{F\_D}$  depends only on the product of size parameter and sine of the truncation angle, that is  $(x \sin \alpha)$ . This truncation error  $T_{F\_D}$  is shown in Fig. 3 for very large (i.e.,  $x = 1000$ ; e.g.,  $d = 175 \mu\text{m}$  at  $\lambda = 0.55 \mu\text{m}$ ) particles. At small angles it is much larger than the truncation errors due to either reflection or transmission, with  $T_{F\_D}(x = 1000, \alpha = 7^\circ) = 99.5\%$ . Consequently, for very large particles only very little of the diffracted light is measured by a nephelometer with a typical forward truncation angle of  $7^\circ$ . Note that this truncation error would be directly applicable only if diffraction constituted the only scattered process. This is approximately the case for large particles and small truncation angles. Otherwise, Eq. (14b) must be used to calculate the compounded truncation error from multiple scattering processes.

## VI. COMPARISONS WITH MIE THEORY

### A. Small particle approximation as function of truncation angle

For the refractive indices used for our Mie calculations, Rayleigh truncation errors [Eq. (5)] agree very well with those from Mie calculation for  $x = 0.1$  as shown in Fig. 2. Mie results converge towards the Rayleigh equation [i.e., Eq. (5)] for  $x \rightarrow 0$ , explaining the identical forward and backward truncation errors independent of refractive index as seen in Fig. 1.

### B. Large particle approximation as function of truncation angle

For very large ( $x = 1000$ ; e.g.,  $d = 175 \mu\text{m}$  at  $\lambda = 0.55 \mu\text{m}$ ) particles, the forward truncation error calculated due to the sum of diffraction, reflection, and transmission shows excellent agreement with Mie theory [Figs. 4(a) and 4(b)]. For small truncation angles, the truncation errors are nearly exclusively caused by diffraction. Even at a typical forward truncation angle of  $7^\circ$ , 96.3% (99.5%) of the Mie truncation error can be ascribed to diffraction for nonabsorbing (absorbing) aerosol. The diffraction truncation error starts saturating at a truncation angle about  $0.2^\circ$ , as the diffraction cross section approaches the geometric cross section  $G$ , which corresponds to a fractional truncation error of 0.5 for nonabsorbing aerosol [Fig. 4(a)]. From about  $0.2^\circ$  to nearly  $10^\circ$ , the truncation error changes little. Above  $10^\circ$ , the contribution of transmission and to a lesser degree reflection becomes significant, with the total scattering cross section approaching  $2G$ , thereby increasing the truncation error to 0.96 at  $90^\circ$ . For very large absorbing aerosols, the transmission has been eliminated and a large majority of the scattered light is due to diffraction with the small remainder being due to reflection. This results in much (nearly a factor of 2) larger forward truncation errors at small angles as diffraction dominates the scattering process in all of Fig. 4(b). This explains the difference in truncation errors for nonabsorbing and absorbing aerosols noticed in Mie calculations (e.g., Fig. 1) and previously noticed by Rosen *et al.*<sup>7</sup>

For smaller particles, diffraction truncation shifts to larger angles since the diffraction truncation error is a function of the product of particle size and the sine of the truncation angle [i.e.,  $x \sin \alpha$ ; see Eq. (21b)], while transmission (for nonabsorbing and strongly absorbing particles) and reflection truncation errors are independent of particle size. For large ( $x = 100$ ; e.g.,  $d = 17.5 \mu\text{m}$  at  $\lambda = 0.55 \mu\text{m}$ ) particles, agreement with Mie calculations remains very good [Figs. 4(c) and 4(d)], while for relatively small ( $x = 10$ ; e.g.,  $d = 1.75 \mu\text{m}$  at  $\lambda = 0.55 \mu\text{m}$ ) particles this agreement begins to deteriorate [Figs. 4(e) and 4(f)]. However, even for relatively small particles (i.e.,  $x = 10$ ) diffraction theory does a reasonable job in describing small angle truncation errors.

### C. Large particle approximation at small angles as function of particle size

The previous section implied that diffraction theory [Eqs. (21b) and Eq. (14b)] might be all that is needed to

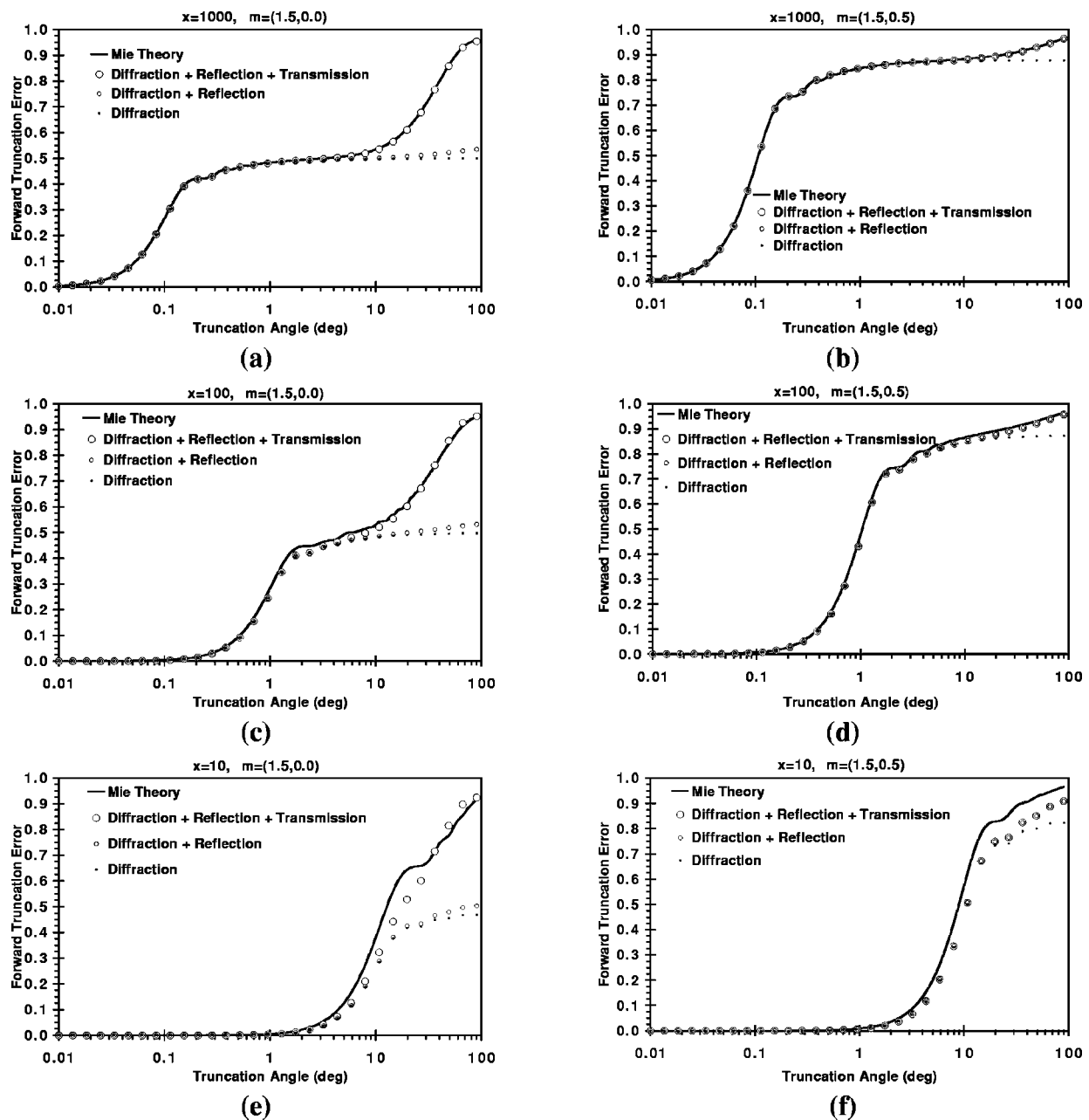
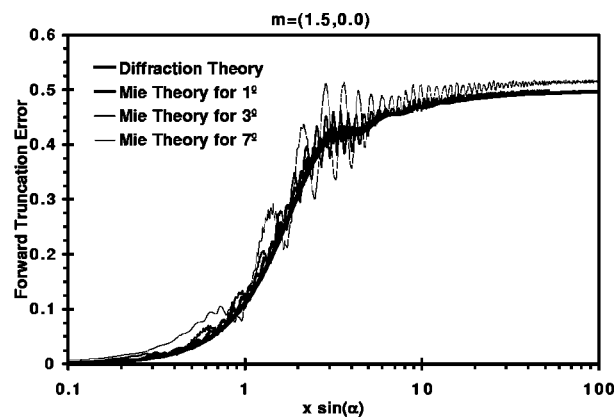


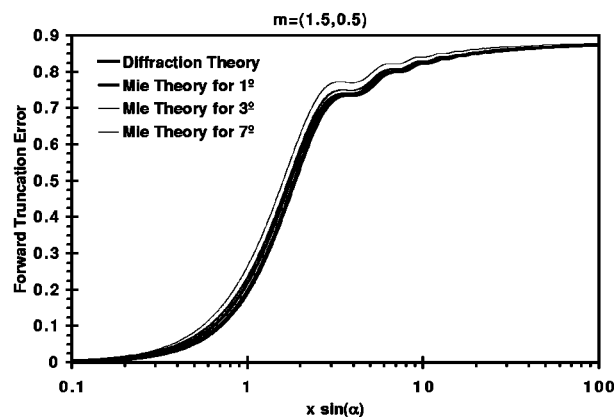
FIG. 4. Forward scattering truncation errors from Mie theory and from diffraction, transmission, and reflection: (a) very large ( $x=1000$ ; e.g.,  $d=175 \mu\text{m}$  at  $\lambda=0.55 \mu\text{m}$ ) nonabsorbing particles; (b) very large ( $x=1000$ ; e.g.,  $d=175 \mu\text{m}$  at  $\lambda=0.55 \mu\text{m}$ ) absorbing particles; (c) large ( $x=100$ ; e.g.,  $d=17.5 \mu\text{m}$  at  $\lambda=0.55 \mu\text{m}$ ) nonabsorbing particles; (d) large ( $x=100$ ; e.g.,  $d=17.5 \mu\text{m}$  at  $\lambda=0.55 \mu\text{m}$ ) absorbing particles; (e) relatively small ( $x=10$ ; e.g.,  $d=1.75 \mu\text{m}$  at  $\lambda=0.55 \mu\text{m}$ ) nonabsorbing particles; and (f) relatively small ( $x=10$ ; e.g.,  $d=1.75 \mu\text{m}$  at  $\lambda=0.55 \mu\text{m}$ ) absorbing particles.

describe forward truncation errors at relative small truncation angles as common in modern integrating nephelometers. This implication is investigated further in the following. Figures 5(a) and 5(b) show a comparison between Mie theory for truncation angles of  $1^\circ$ ,  $3^\circ$ ,  $7^\circ$ , and diffraction theory [Eq. (21b)] both for nonabsorbing [Fig. 5(a)] and absorbing [Fig. 5(b)] particles. Both Mie and diffraction results are plotted as function of the product of size parameter  $x$  and sine of truncation angle (i.e.,  $x \sin \alpha$ ) with the  $x \sin \alpha$  scale ranging from 0.1 to 100. The corresponding size parameter scales range from 5.730 to 5730 ( $\alpha=1^\circ$ ), 1.911 to 1911 ( $\alpha=3^\circ$ ), and 0.8206 to 820.6 ( $\alpha=7^\circ$ ). For these small angles, appropriate for modern nephelometers, diffraction theory is suitable to estimate relevant truncation errors. It does not reproduce the

rapid oscillations that Mie theory yields for nonabsorbing particles. However, these oscillations average out for common particle size distributions anyway. For large particles, as the truncation angle increases the contributions of reflection and transmission (for nonabsorbing particles) become significant and diffraction theory predicts a smaller truncation error than Mie theory. This can be seen in Fig. 5 for  $\alpha=7^\circ$ , where at large  $x \sin \alpha$ , the Mie theory prediction is barely larger for absorbing particles where only reflection adds to the diffraction truncation error [Fig. 5(b)], but somewhat larger for nonabsorbing particles where both reflection and transmission are added [Fig. 5(a)]. For very small particles, diffraction theory is not appropriate to describe truncation errors. However, in this Rayleigh regime, truncation



(a)



(b)

FIG. 5. Forward scattering truncation errors from diffraction theory and from Mie theory at small angles: (a) nonabsorbing particles; and (b) absorbing particles.

errors are quite small and the even simpler Rayleigh theory can be used as discussed in a previous section.

While truncation errors for nonspherical particles have not been calculated here, the “geometric optics plus diffraction” treatment used can readily be generalized to nonspherical particles of known shape. It is expected that for most large nonspherical atmospheric particles truncation errors will be dominated by diffraction and can be evaluated by solving the appropriate diffraction integral. Possible exceptions are particles with parallel surfaces oriented perpendicular to the direction of incident light, such as oriented ice platelets, where transmitted light would contribute significantly to the truncation error.

## VII. DISCUSSION

To understand nephelometers truncation errors, one needs to be aware of the scattering phase functions of both calibration media and the particles of interest. In the ideal, but totally unrealistic case, these phase functions are identical, and truncation errors can be eliminated. In practice, calibration media are gases with their well-known Rayleigh phase function, resulting in small truncation errors, while the particles of interest have an unknown size distribution resulting in poorly constrained truncation errors.

At a given truncation angle, truncation errors depend both on the particle’s size and complex refractive index. For large particles most of the light scattered into the near forward direction is due to diffraction and dominates truncation errors. For typical truncation angles of about  $7^\circ$ , it has been shown that for relatively large particles (i.e., diameter larger than three times the wavelength) truncation errors are well described by diffraction theory alone.

For relatively large absorbing particles, it has been shown that forward truncation errors are nearly a factor 2 larger than for nonabsorbing particles due to the suppression of transmitted light, resulting in a larger contribution of forward-peaked diffraction to the scattering phase function.

## ACKNOWLEDGMENTS

It is a pleasure to thank Dr. Peter W. Barber for a critical reading of the manuscript. This research was supported in part by the National Science Foundation under Grant No. ATM-9871192, and by the Applied Research Initiative of the State of Nevada.

- <sup>1</sup>N. C. Ahlquist and R. J. Charlson, *J. Air Pollut. Control Assoc.* **17**, 467 (1967).
- <sup>2</sup>R. G. Beuttell and A. W. Brewer, *J. Sci. Instrum.* **26**, 357 (1949).
- <sup>3</sup>R. J. Charlson, H. Horvath, and R. F. Pueschel, *Atmos. Environ.* **1**, 469 (1967).
- <sup>4</sup>J. Heintzenberg and R. J. Charlson, *J. Atmos. Ocean. Technol.* **13**, 987 (1996).
- <sup>5</sup>G. H. Ruppertsberg, *Beitr. Phys. Atmos.* **37**, 252 (1964).
- <sup>6</sup>T. L. Anderson *et al.*, *J. Atmos. Ocean. Technol.* **13**, 967 (1996).
- <sup>7</sup>J. M. Rosen, R. G. Pinnick, and D. M. Garvey, *Appl. Opt.* **36**, 2642 (1997).
- <sup>8</sup>T. L. Anderson and J. A. Ogren, *Aerosol Sci. Technol.* **29**, 57 (1998).
- <sup>9</sup>D. S. Ensor and A. P. Waggoner, *Atmos. Environ.* **4**, 481 (1970).
- <sup>10</sup>J. Heintzenberg and H. Quenzel, *Atmos. Environ.* **7**, 503 (1973).
- <sup>11</sup>H. Quenzel, *Gerlands Beitr. Geophys.* **78**, 251 (1969).
- <sup>12</sup>H. Quenzel, G. H. Ruppertsberg, and R. Schellhase, *Atmos. Environ.* **9**, 587 (1975).
- <sup>13</sup>R. A. Rabinoff and B. M. Herman, *J. Appl. Meteorol.* **12**, 184 (1973).
- <sup>14</sup>J. W. Fitzgerald, *J. Appl. Meteorol.* **16**, 198 (1977).
- <sup>15</sup>R. Varma, H. Moosmüller, and W. P. Arnott, *Opt. Lett.* (to be published).
- <sup>16</sup>H. Horvath, *Atmos. Environ.* **7**, 521 (1973).
- <sup>17</sup>H. Horvath and W. Kaller, *Atmos. Environ.* **28**, 1219 (1994).
- <sup>18</sup>M. A. Peñalosa M., *Meas. Sci. Technol.* **10**, R1 (1999).
- <sup>19</sup>E. M. Patterson, B. A. Bodhaine, A. Coletti, and G. W. Grams, *Appl. Opt.* **21**, 394 (1982).
- <sup>20</sup>M. Jonasz, *Appl. Opt.* **29**, 64 (1990).
- <sup>21</sup>G. Mie, *Ann. Phys. (Leipzig)* **25**, 377 (1908).
- <sup>22</sup>W. J. Wiscombe, *Appl. Opt.* **19**, 1505 (1980).
- <sup>23</sup>C. F. Bohren and D. R. Huffman, *Absorption and Scattering of Light by Small Particles* (Wiley, New York, 1998).
- <sup>24</sup>A. A. Kokhanovsky and E. P. Zege, *J. Aerosol Sci.* **28**, 1 (1997).
- <sup>25</sup>W. T. Grandy, *Scattering of Waves from Large Spheres* (Cambridge University Press, New York, 2000).
- <sup>26</sup>J. H. Seinfeld and S. N. Pandis, *Atmospheric Chemistry and Physics: From Air Pollution to Climate Change* (Wiley, New York, 1998).
- <sup>27</sup>H. Gerber, Y. Takano, T. J. Garrett, and P. V. Hobbs, *J. Atmos. Sci.* **57**, 3021 (2000).
- <sup>28</sup>S. Chandrasekhar, *Radiative Transfer* (Dover, New York, 1960).
- <sup>29</sup>A. Bucholtz, *Appl. Opt.* **34**, 2765 (1995).
- <sup>30</sup>H. C. van de Hulst, *Light Scattering by Small Particles* (Dover, New York, 1981).
- <sup>31</sup>J. A. Lock and L. Yang, *J. Opt. Soc. Am. A* **8**, 1132 (1991).
- <sup>32</sup>K.-N. Liou and J. E. Hansen, *J. Atmos. Sci.* **28**, 995 (1971).
- <sup>33</sup>J. E. Hansen and L. D. Travis, *Space Sci. Rev.* **16**, 527 (1974).
- <sup>34</sup>J. R. Hodkinson and I. Greenleaves, *J. Opt. Soc. Am.* **53**, 577 (1963).